NASA

Technical Memorandum 85005

Large Amplitude MHD Waves Upstream of the Jovian Bow Shock

M. L. Goldstein, C. W. Smith, and W. H. Matthaeus

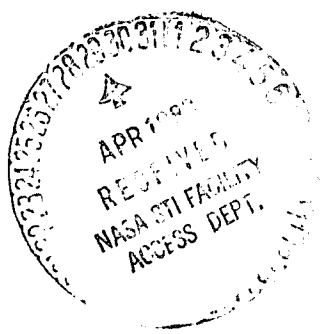

MARCH 1983

National Aeronautics and Space Administration

Goddard Space Flight Center
Greenbelt, Maryland 20771

LARGE AMPLITUDE MHD WAVES UPSTREAM OF THE JOVIAN BOW SHOCK

by

Melvyn L. Goldstein
Laboratory for Extraterrestrial Physics
Code 692, NASA/Goddard Space Flight Center
Greenbelt, MD 20771

Charles W. Smith
Space Science Center
Department of Physics
University of New Hampshire
Durham, NH 03824

and

William H. Matthaeus
Department of Physics and Astronomy
University of Maryland
College Park, MD 20742

SUBMITTED TO: The Journal of Geophysical Research

Abstract

Observations of large amplitude MHD waves upstream of Jupiter's bow shock are analyzed. The waves are found to be right circularly polarized in the solar wind frame which suggests that they are propagating in the fast magnetosonic mode. A complete spectral and minimum variance eigenvalue analysis of the data was performed. The power spectrum of the magnetic fluctuations contains several peaks. The fluctuations at 2.3 mHz have a direction of minimum variance along the direction of the average magnetic field. Several harmonics at 6, 9, and 12 mHz are also present. The direction of minimum variance of these fluctuations lies at approximately 40° to the magnetic field and is parallel to the radial direction (toward the sun). We argue that these fluctuations are waves excited by protons reflected off the Jovian bow shock. The inferred speed of the reflected protons is about two times the solar wind speed in the plasma rest frame. A linear instability analysis is presented which suggests an explanation for many of the observed features of the observations. That analysis also predicts that the fluctations contain a significant fraction of magnetic energy that is linearly polarized and in the Alfven mode.

1. Introduction

As Voyager 2 approached Jupiter, the interplanetary magnetic field was oriented out of the ecliptic plane for several days. The orientation was such that Voyager traversed the foreshock region from the downstream side. This fortuitous geometry resulted in the detection of a series of upstream wave events reminiscent of the phenomenon studied so intensively at earth. The general characteristics of these events have been discussed in detail by Smith, Goldstein, and Matthaeus [1983].

The purpose of this paper is to analyze the last of the events encountered by Voyager. For several reasons this last event appears to be very young in that it may represent an early stage in the wave-particle interaction between the interplanetary magnetic field and solar wind protons reflected from the bow shock. This event was very brief, lasting only 1 1/2 hours. During this time, the direction of the interplanetary magnetic field was connected to the Jovian bow shock and was oriented out of the ecliptic plane at a 45° angle. In this paper we present an analysis of the magnetic field and plasma data taken during this interval. We find that the enhanced magnetic fluctuations are grouped into a few frequency bands (four or five), and that in each frequency band, the fluctuations have nearly circular polarization which is right-handed in the solar wind frame of reference. At least at the lowest frequencies, where the relevant plasma data is available, the waves are propagating outward from the bow shock. Furthermore, the wavevectors tend to be more field aligned at the lowest frequencies than at higher ones. The various frequency bands are in approximate harmonic relationship to each other. We conclude that the waves are probably in the fast magnetosonic

branch (but the possiblity of a sizable contribution from linearly polarized Alfven mode fluctuations at the higher harmonics cannot be ruled out). We have inferred the velocity of the plasma particles which can resonanate with these waves. We find that the observations are consistent with excitation by protons streaming away from the bow shock at about the solar wind speed. Similar observations of upstream waves have been made at earth [see, for example, Hoppe et al., 1981], but to our knowledge the harmonic structure reported here has not as yet been reported in the near earth environment. The resonant velocity deduced for these reflected protons is consistent with the recent simulations of oblique shocks by Leroy et al. [1982] and Tanaka et al. [1983].

In §2 we discuss the observations and the spectral analysis of the magnetic field and plasma data which motivates the interpretation presented in §3. In §4 we develop that interpretation further by presenting a linear wave-particle instability analysis in which we show that a distribution function of solar wind protons (orginating by reflection from the Jovian bow shock) can, in principle, generate the fundamental and harmonics observed in the power spectrum. The direction of maximum growth for the fast magnetosonic mode is found to be close to the observed minimum variance direction in all cases. Additional limitations of this analysis and a summary are given in §5.

2. Wave Mode Identification

The time period of interest is the interval from about 9:00 to 10:30 UT on day 184 of 1979. A plot of the magnetometer data taken by the GSFC experiment [see Behannon et al., 1977 for a description of the experiment] is shown in Figure 1. The data have been rotated to the mean field coordinate system with

the z-axis along the mean field direction. During this time the components of the average magnetic field (in the usual RTN coordinate system) were (0.229, 0.0382, 0.195) nT, respectively. The x-direction is in the R-T plane. The fluctuations in all three components and in the magnitude are large, $\delta B_{rms} \approx 1.3|\langle \underline{B}_o \rangle|$, but appear to be dominated by only a few frequencies.

The quasi-monochromatic appearance of the data is somewhat deceptive. In Figure 2a we show the power spectrum of this interval. This spectrum is constructed using the fast Fourier transform technique and has 14 degrees of freedom. The data, consisting of 1.92 sec averages of the magnetic field, was digitally filtered with a low pass filter to eliminate aliasing at the highest frequencies. Because the spectrum is falling so steeply, there is a possibility that "leakage" from the strong peak near 3 mHz might be distorting the spectrum above about 12 mHz. This possibility was investigated by "prewhitening" the data. We found that above about 12mHz the spectrum is, in fact, distorted by leakage, but the peaks in the spectrum at 12 mHz and below are preserved in the prewhitened data.

The spectrum is striking for the presence of several large peaks. The largest is centered near 2.3 mHz and several smaller peaks are visible at higher frequencies. The high frequency peaks in the sprectrum out to 9 or 12 mHz appear to be in approximately a harmonic relationship with a fundamental at 2.3 mHz. The first two peaks in the spectrum are statistically significant while the significance of the higher "harmonics" is not as certain, and above 12 mHz no statistical significance can be ascribed to the spectrum.

During this period the solar wind velocity, kindly provided to us by the Voyager PLS team [see Bridge et al., 1977 for a description of the experiment], was in the radial direction with a magnitude of 420 km/s. At the end of this interval it dropped to 400 km/s. The proton density fluctuated

between 0.1 - 0.4 protons/cm^3 with an average of 0.2. The electron temperature was approximately 2-3 eV (E. Sittler, private communication).

Smith et al. [1983] have shown that for MHD fluctuations in a super-Alfvenic flow, the sense of polarization in the plasma frame can be obtained from a determination of the magnetic helicity [see Moffatt, 1978; Matthaeus and Goldstein, 1982a]. In Figure 3 we have plotted the normalized magnetic helicity spectrum $\sigma_m(f)$ as defined in Matthaeus and Goldstein [1982a] and Smith et al. [1983]. The first thing to note about the helicity spectrum is that in the vicinity of the spectral peaks it is nearly positive definite and attains nearly 80% of its maximally allowed value of ± 1, implying that the flucutations are nearly circularly polarized. This magnetic helicity spectrum is distinct from spectra normally seen in interplanetary regions far removed from planetary bow shocks and the reader is referred to Matthaeus and Goldstein [1982a] for comparison spectra taken in the ambient solar wind. For this interval $\langle B_R \rangle > 0$ and the fluctuations therefore have right-handed polarization in the plasma frame.

From an eigenvalue analysis of this time interval, the degree of polarization and ellipticity of these fluctuations can be determined. At each Fourier mode the spectral matrix is rotated into an eigenvalue coordinate system in which the smallest eigenvalue is associated with the direction of the minimum variance of the fluctuations. In Figure 4 we show some of the results of this calculation. The degree of polarization D, the ellipticity ϵ, and the angle θ between $\underline{B}_o$ and $\underline{k}$, the direction of minimum variance, are plotted versus frequency. We will assume that the direction of minimum variance corresponds, within a sign, to the physical direction of propagation of the wave phase velocity. It is clear that the normalized helicity and degree of polarization track each other very well and that the ellipticity is large when σ_m is large.

This confirms that the fluctuations are nearly circularly polarized. Subject to the constraint that the fluctuations have phase speeds less than the solar wind speed, then the waves are right circularly polarized in the plasma frame. Note that θ is 10° at the lower frequencies ($\simeq$ 2.5 mHz) but increases to about 40° at the higher harmonic peaks ($\simeq$ 6, 9, and 12 mHz). Although not obvious in the power spectra (Fig. 2), the plots of σ_m, D and ϵ suggest that the harmonic structure may also extend to 15 or 18 mHz (cf. Figs. 3 and 4). Because the spectrum in this range in not statistically significant, we confine our attention in the following discussion to the spectrum below 15 mHz.

Because θ is significantly smaller at frequencies near 3 mHz than it is at the higher frequences, one might expect that the low frequency modes are less "compressive" than are the higher frequency ones. This would be particularly true if the fluctuations were fast mode waves as is suggested by the fact that the rest frame polarization is right-handed. Fast mode waves should show significant power in the spectrum of the magnitude of $\underline{B}$, except for propagation nearly parallel to the mean field when they become degenerate with Alfven waves (if the Alfven speed exceeds the sound speed). Thus we might expect that the power spectrum of the magnitude of $\underline{B}$ would have suppressed power near 2.5 mHz, but would still contain the large peaks in the spectrum seen in Figure 2a. This is confirmed in Figure 2b where the power in $|\underline{B}|$ is plotted. Note that the spectrum has no peak at 2.5 mHz, but does contain the higher frequency harmonics seen in the spectrum of the components (2a).

The degree of compression in these fluctuations can also be examined using the proton density measurements. Fast mode waves normally show a strong correlation between $|B|$ and ρ. However, in this case, where we suspect that the fundamental is propagating nearly parallel to B_o, the correlation should be weak because of the degeneracy with the Alfven branch. The higher harmon-

ics are propagating at larger angles and should show stronger correlations between |B| and ρ. Because of the sampling limitations of the plasma instrument (one sample every 96s), only the correlation near the fundamental can be examined. In Figure 5a we have plotted the correlation between |B| and ρ defined following Smith et al. [1983]. As expected, the correlation is weak near 2.5 mHz and is consistent with being zero. In this case, in contrast to the work of Gary et al. [1981], the waves, although apparently in the fast magnetosonic mode, are noncompressive and are propagating parallel to $\langle \underline{B} \rangle$ at these lower frequencies. We return to this point below when discussing the excitation of such waves by wave-particle resonances.

The directions of propagation cannot be resolved solely from an eigenvalue analysis. However, at the low frequency end of the spectrum, the cross helicity [cf. Matthaeus and Goldstein, 1982a] can be used to resolve the ambiguity in the sign of the propagation direction. In Figure 5b, we have plotted the normalized cross helicity σ_c, as defined by Matthaeus and Goldstein. Although very few degrees of freedom are available for such a short data set, the cross helicity spectrum is positive and quite large near 2.5 mHz. The positive sign of σ_c indicates that "Alfvenic" fluctuations (including fast mode waves) are propagating antiparallel to the mean field direction, i. e. outward, away from Jupiter (recall that $\langle B_R \rangle > 0$). Furthermore, the fact that there is significant cross helicity in this frequency range is further evidence that the fluctuations are MHD and not whistlers. (The velocity determination in this analysis includes only ion data.)

The Alfven ratio r_A, which is the ratio of the spectrum of kinetic energy to that of magnetic energy, is plotted in Figure 5c. For MHD fluctuations, r_A is expected to be close to one, while for whistler waves, r_A would be nearly zero. Note that near 3 mHz r_A is close to unity, providing further evidence

that these fluctuations are MHD.

Another consistency check on the fast mode identification is to compute the ratio of the Alfven to sound speeds during this time. The large amplitudes of the magnetic fluctuations and the relatively large value of the cross helicity together with the nearly field aligned direction of minimum variance, suggest that the fast mode is nearly degenerate with the Alfven branch. This can occur if θ is nearly zero and if $V_A > C_s$, where V_A and C_s are the Alfven and sound speeds, respectively. E. Sittler has kindly provided us with the electron temperature for this interval so that C_s can be estimated. If we assume that the electrons are isothermal ($\gamma = 1$), then C_s and V_A are approximately given by

$$C_s = \sqrt{(T_e/m_i)} \tag{1}$$

and

$$V_A = B_o/\sqrt{(4\pi\rho)} \tag{2}$$

where T_e is the electron temperature in eV, m_i is the proton mass, ρ is the ion mass density, and B_o is the mean magnetic field strength. Using $T_e = 2$ eV, C_s is 1.38×10^6 km/s while $V_A = 1.44 \times 10^6$ km/s. The difference between these numbers is not significant because of experimental uncertainties and the approximations made in writing (1) and (2). These results, while not proving that $V_A > C_s$, is at least not inconsistent with the assertion that we are observing fast mode waves.

We now feel justified in concluding that the portion of these fluctuations that is elliptically polarized is right-handed in the plasma frame and is

propagating away from the Jovian bow shock in the fast magnetosonic mode. The remainder of this analysis is based on this conclusion.

3. Source of the Waves

From the eigenvalue analysis we know both the direction of $\underline{k}$ with respect to $\underline{B}_o$ as well as ϕ, the direction of $\underline{k}$ with respect to $\underline{V}_{SW}$. Thus the plasma frame frequency of these waves can be computed. In Table 1 we have listed the angle between $\underline{k}$ and $\underline{B}_o$, $\underline{k}$ and $\underline{V}_{SW}$, and the rest frame frequency for the Fourier modes contained in the power spectrum (Figure 2a).

We are now in a position to examine the possibility that these waves are amplified by wave particle resonances. The linear, or even quasilinear, theory of wave-particle resonances is a small wave amplitude theory and, as discussed above, these fluctuations clearly have rather large amplitudes. Thus we are probably in a nonlinear regime and no theory of the dispersion characteristics of nonlinear compressive MHD modes exists [see Barnes, 1979 for a review]. Nonetheless, we will show below that if one proceeds on the assumption that linear theory sometimes yields valuable information even in parameter regimes where its use is probably not formally justified, some insights can be gleaned about the possible origin of these fluctuations.

To continue, we make several basic assumptions. In the next section, we impose additional approximations and treat the problem in the context of linearized Vlasov-Maxwell theory. First we assume that the relationship between ω, the rest frame frequency (in radians/s), and $\underline{k}$ will be given approximately by the linear dispersion relation for the magnetosonic fast mode. (We will see in the next section that even this assumption almost certainly requires modification at the lowest frequencies in the spectrum.)

One can then solve for the resonant velocity. Since the dispersion relation cannot be independently determined from single point measurements, the most that can be obtained from such a procedure is a internally consistent picture of the interaction.

From the Doppler shift calculation made in §2 (see Table 1), we see that the rest frame frequencies are well below the proton cyclotron frequency of 6 mHz, as expected for MHD waves. Even the 4th harmonic at 12 mHz has a rest frame frequency of only 0.6 mHz.

The fast mode dispersion relation can be written as [Boyd and Sanderson, 1969, p. 188]

$$(\omega/k)^2 = (1/2)\{(C_s^2 + V_A^2) + [(C_s^2 + V_A^2)^2 - 4C_s^2V_A^2\cos^2\theta]^{1/2}\} \qquad (3)$$

Using (3), k can be calculated. Since both θ and ϕ are known from the eigenvalue analysis, the wave-particle resonance condition

$$v_{\parallel} = (\omega - n\Omega_p)/k\cos\theta \qquad (4)$$

can be solved for $v_{\parallel}$ ($\Omega_p = eB/m_pc$ is the proton Larmor frequency and e is the magnitude of the electron charge). For frequencies near 2 - 3 mHz, we let n = 1 with the result that $v_{\parallel} \approx -2V_{SW}$ (Table 1), where we have assumed that the resonant particles are protons. For frequencies corresponding to the second harmonic in the spectrum at 6 mHz (Fig. 2), we set n = 2; again, $v_{\parallel} \approx -2V_{SW}$. Similary, for the third and fourth harmonics near 9 and 12 mHz, we let n = 3 and 4, respectively. Again, $v_{\parallel} \approx -2V_{SW}$ (Table 1). Note that ions heavier than protons resonate with lower frequencies and have even slower resonant velocities. Thus it appears unlikely that these fluctuations could be excited

by heavy ions of magnetospheric origin. We think our conclusion that the observed fluctuations are excited by reflected protons is strongly supported by this simple analysis. The linear instability analysis described below is predicated on this assumption.

4. Linear Analysis

In this section we treat the excitation of these upstream waves as arising from an electromagnetic ion beam instability. This instability has been considered previously in an astrophysical context by Tademaru [1969] and as an explanation of double ion beams in the solar wind by Montgomery et al. [1975; 1976], Abraham-Schrauner et al. [1979] and Gary [1978], among others. The instability has also been invoked to explain excitation of MHD waves upstream of the terrestrial bow shock by Barnes [1970] and most recently by Gary et al. [1981] and Lee [1981], to name a few. Previous analyses of near earth phenomena have been confined to examining excitation of the $n = 1$ resonance. Harmonics have not as yet been investigated in terrestrial studies. The work of Tademaru [1969] contains the complete formalism including all harmonics, but is replete with both typographical and algebraic errors. We have rederived the growth rate following Tademaru's approach and use our results in this section.

The first problem is that of deciding on the form of the ion distribution. Based on our preliminary analysis in §3, we assume that the ions are low energy protons detectable only by the PLS instrument on Voyager. Their energy would be only a few keV in the spacecraft frame. The viewing geometry for detecting such a particle population is very unfavorable. The four Faraday cups which comprise the PLS instrument were pointed toward earth while the

reflected particles were coming from the opposite hemisphere. Nonetheless, we have searched the PLS data for evidence of these reflected protons. During virtually the entire period the angle between the instantaneous magnetic field (in spacecraft coordinates) and the look directions of the four cups was such that it was extremely improbable that these particles could be seen. The density of these reflected particles is expected from similar observations at earth to be only a small fraction (of order 1%) of the solar wind density [Bonifazi and Moreno, 1981; Paschmann, et al., 1980; 1981], which would reduce the signal to noise ratio. An additional consideration is that the pitch angle of the reflected beam and the width of that distribution are unknown. Therefore it is not altogether surprising that our search through the plasma data did not reveal any unequivocal evidence of reflected protons.

Finally, the possibility should be kept in mind that the particles exciting the waves were in fact not present during this time. The waves could have been created somewhat earlier in a different region of space so that we were observing only the waves. The damping of Alfvenic fluctuations would be weak and even the higher harmonic magnetosonic modes might survive long enough to be observed because we find that Landau damping of these waves is not very significant at the inferred angles of propagation.

We have, therefore, postulated a distribution function which we believe is both consistent with our conclusions in §3 and with observations and computer simulations of the similar phenomenon seen near earth. We take the streaming proton distribution to be a two-temperature streaming Maxwellian of the form

$$f(v_\perp, v_\parallel) = (n_b/n_o)(\pi^{3/2} V_\perp^2 V_\parallel)^{-1} \exp(-v_\perp^2/V_\perp^2) \exp-[(v_\parallel - V_s)^2/V_\parallel^2] \qquad (5)$$

where $V_\perp$ and $V_\parallel$ are the perpendicular and parallel (with respect to $\langle \underline{B} \rangle$)

thermal spread of the streaming protons and V_s is the streaming velocity which we take to be 1.8 V_{sw} based on examination of Table 1. Tanaka et al. [1983] concluded that their simulations and the observations of Bonifazi and Moreno [1981] and Paschmann et al. [1981] were most consistent with $(n_b/n_o) \simeq 0.01$, $V_\parallel$ of order 0.2 V_{sw} and $V_\perp$ of order 2 - 3 $V_\parallel$.

We will not present results of a complete parameter search for our analysis, but will show our conclusions only for that choice of parameters that seemed to best match the observations. The greatest discrepancy we found between parameters that seemed to work at earth and those that gave the best results in our linear analysis was that $V_\perp$ needed to be as much as $6V_\parallel$ to produce maximum growth in the observed direction. All other parameters were chosen to be the ones mentioned above from Tanaka et al. [1982] and Paschmann et al. [1981]. The much higher ratio of $T_\perp/T_\parallel$ in our analysis may arise from the fact that the solar wind is cooler at Jupiter than at 1 AU but the streaming speed is about the same. The perpendicular thermal velocity of the reflected ions is acquired by transforming the streaming speed into large pitch angle gyromotion which is then thermalized, whereas the parallel thermal velocity essentially arises from the thermal velocity of the solar wind. Thus the necessity of using a larger value of $T_\perp/T_\parallel$ is not too unexpected.

We also included Landau damping by both thermal solar wind protons and electrons. We used a solar wind temperature of 2 eV for both components and the measured density of 0.207 particles/cm^3. The thermal protons were generally unimportant, but Landau damping by electrons is significant at large propagation angles at the higher harmonics. The expression for the growth rate γ is given in Appendix A.

For the parameters given above, the proton distribution (5) is very unstable. For the fundamental we found that γ/Ω_p exceeded unity, violating

the Taylor series expansion used in deriving (A1). However, because maximum growth is along $\underline{B}_o$, an expression for γ valid for parallel propagation can be easily derived in which both ω and γ are solved for simultaneously [see, for example, Lee 1981]. When using this expression, the real part of the frequency is significantly modified, and the phase speed is now up to twenty times the Alfven speed (cf. Table 2) for the parameters we have used. This behavior of the linear analysis arises from the very large growth rates which result from our choice of parameters. For example, choosing a smaller value for n_b/n_o would lessen this effect.

At the higher harmonics, γ/Ω_p is less than one, and equations (A1) and (A2) can be used. The results of the calculations are summarized in Table 2. The first thing to note is that the growth rates for the fundamental, second and third harmonics are all large which is consistent with the observed large amplitude of these fluctuations and with the fact that the power spectral peaks for the fundamental and second peaks are of comparable magnitude. The maximum growth rate of the fundamental occurs at $\theta = 0$, consistent with the minimum variance result of $\theta \simeq 10°$. (As noted by Gary et al. [1981], and also found in our own calculations, the growth rate is still substantial at larger angles, up to 20° or more and is actually quite flat out to about 5°. This may be related to the fact that the minimum variance direction is not quite 0.) Finally, note that the higher harmonics all have maximum growth close to $\theta \simeq 40°$, again consistent with the minimum variance analysis summarized in Table 1.

At propagation angles different from zero, it becomes possible to excite the Alfven branch in addition to the fast mode. In the context of the formula for the growth rate, (A2), this entails changing the sign of n and ω while leaving the sign of $k_{\parallel}$ unchanged. With n = +1, the growth rate of the Alfven

mode is less than that of the fast mode for all propagation angles of interest. However, for $n > 1$, the maximum growth rate of the Alfven mode (maximized with respect to $\underline{k}$), actually exceeds the growth rate of the fast mode wave. Maximum growth occurs at a larger angle, close to 50° (see Table 2). This large growth is perhaps surprising, but one should keep in mind that these waves are nearly linearly polarized (cf. Table 2), which enables resonance with streaming protons to occur, and, unlike the fast mode waves, the Alfven waves are essentially unaffected by Landau damping.

At this point we must question of the relationship of this analysis to the minimum variance results. In using the miniumum variance technique we have assumed that the direction of minimum variance is parallel to $\underline{k}$. However, for linearly polarized fluctuations, there is no direction of minimum variance. Hence, because fast mode waves are also excited and are right elliptically polarized, the minimum variance direction found will be associated with the fast mode fluctuations. The power spectrum, however, will contain contributions from both modes since the parallel components of $\underline{k}$ are approximately equal in both cases. The larger growth rates of the Alfven mode may then account for the relatively large spectral peaks at 9 and 12 mHz.

Having said all this, we must interject the caveat that the observed fluctuations almost certainly represent the result of nonlinear processes, and arguments based on linear theory should be accepted only with some caution. For example, the degree of polarization deduced from the eigenvalue analysis is much greater than would be expected for linear cold plasma fast modes propagating in the direction of minimum variance (cf. Table 2). Another limitation to keep in mind is that we have used the cold plasma dispersion relations in §4. This ignores any effects due to the non-zero sound speed, which as we have seen has approximately the same magnitude as the Alfven speed.

That the ion beam instability can, in principle, excite both the Alfven and fast mode branches is apparently not well known. Recently, Hoppe and Russell [1983] have reported evidence from ISEE 1 and 2 data for Alfven mode fluctuations in the earth's foreshock. They concluded that these fluctuations must be excited by a diffuse distribution of upstreaming protons because the Alfven mode could not be amplified by an ion beam. As we have seen, this is not correct, and while the fluctuations analyzed by Hoppe and Russell may have been produced by a diffuse ion population, the possiblity that they originated from a reflected ion distribution should not be ignored. The more evolved the interaction is, the greater is the probability that Landau damping will have preferentially removed the fast mode component leaving only the linearly polarized Alfven mode fluctuations.

Considering the limitations of linear theory the success of this analysis in explaining the observations suggests that although the waves are observed with large fluctuation amplitudes, the initial excitation may well have been via the electromagnetic ion beam instability. Subsequent evolution has apparently preserved the directions of maximum growth of the fast mode component and also reflects the comparable growth rates for the first several harmonics.

5. Discussion

The analysis we described in §§3 and 4 make use of the assumption, fundamental to the use of any resonance condition at all, that the particle distributions are gyrotropic, i. e. uniform in phase about the mean field, $\underline{B}_o$. The wave spectra excited by such distributions must themselves be gyrotropic. For the higher harmonics, this means that the $\underline{k}$-vectors are distributed in a

cone about the mean field. In realistic cases, resonance broadening will reduce the sharpness of the spectrum of excited waves. However, even in the case of a perfectly sharp wave-particle coupling mechanism there appear to be several effects which might spread the observed wave spectrum.

First, the mean field direction may not be a very well determined statistical quantity. Loosely speaking, waves in different subintervals may be resonant at different angles with respect to a fixed reference direction. To the extent that this is so, the data is neither time stationary nor spatially homogeneous, which would indicate a breakdown of the basic assumptions underlying the simple wave-particle theory used above. To estimate the magnitude of this effect we utilized a 'stationarity test' of the type described by Matthaeus and Goldstein [1982b]. This affords an estimate of the stability of estimates of the mean field from a finite data set. The correlation length for this data set is quite small, $\approx 4.3 \times 10^9$ cm, and the data interval includes ~80 correlation lengths. Thus, not surprisingly, the stationarity test indicated that the mean field direction is, in fact, rather well determined during this data interval.

A second point is that the spectra we have used in characterizing the data are reduced wavenumber spectra depending only on heliocentric radial wavenumber, while the cylindrically symmetric spectra expected from a sharp resonance effect are two dimensional. Unless the mean field is strictly radial, a sharp spectrum of waves produced by wave particle couplings will appear spread over radial wavenumbers.

It might, therefore, seem surprising that the power spectrum shown in Figure 2 is made up of well resolved peaks that have not been completely obliterated by the Doppler shift into the spacecraft frame. This problem was first brought to our attention by M. Lee (private communication). The

essential fact is that the power spectra determined in the super-Alfvenic solar wind are reduced spectra [see, Batchelor 1970]. They are integrated over the two directions perpendicular to the solar wind flow velocity. In Appendix B we show that when a conical distribution of $\underline{k}$-vectors is integrated over these two directions, the resulting reduced spectrum is peaked at two wavenumbers; one at very small $k_{\parallel}$, the second close to the resonance wave number.

The general picture we have is that during this time the interplanetary magnetic field was connected to the Jovian bow shock in such a way that solar wind protons reflected from the shock were able to propagate upstream. This can only happen for oblique or quasi-parallel geometries. From the work of Barnes [970], Gary et al. [1981] and Lee [1981], it is known that such reflected particle distributions can excite fast magnetosonic mode waves. Our analysis of the magnetic field and plasma data has shown that the observed fluctuations are quite probably of this variety, but with an additional contribution of linearly polarized Alfven mode waves which cannot be detected in the eigenvalue analysis. The observation of three or more harmonics in the power spectrum has not been commonly observed before, but the customary explanation in terms of excitation by the electromagnetic ion beam instability does seem to generalize in a straightforward way to include the existence and propagation direction of these higher harmonics.

The phenomenon analyzed here closely resembles similar observations at earth. The alternative possibility, that these waves are related to those observed by the Pioneer spacecraft enroute to Jupiter [Smith et al., 1976] does not, in our view, fit the observations. Smith et al. concluded that the MHD fluctuations that they observed were excited by relativistic electrons via the electron cyclotron instability [Dawson and Bernstein, 1958]. Such cannot

be the case here, because the electron instability excites the Alfven branch and would therefore be left-hand polarized in the 2.3 mHz fundamental, contrary to our observations (cf. Figs. 3, 4, and 5b).

The scenario we have described strikes us as being a rather suggestive one, but, of course, does not constitute a complete description of the phenomenon. For one thing, the particle distribution we used is at best an educated guess based on terrestrial observations and simulations of the earth's bow shock. Observation and analysis of a similar harmonic structure in front of the earth's bow shock will probably go a long way in furthering our understanding of such waves.

Acknowledgments: This work was supported, in part, by the NASA Solar Terrestrial Theory Program grant to the Goddard Space Flight Center. In addition, the work of C. Smith was supported, in part, by the NASA STTP grant to the Univ. of New Hampshire. The authors would like to express their appreciation to K. Behannon, E. Sittler, J. Belcher, M. Acuna, L. Burlaga, and M. Lee for many stimulating discussions. The authors also want to thank both the plasma and magnetometer teams on the Voyager spacecraft, and in particular to the principal investigators, H. Bridge and N. F. Ness, for their encouragement during the course of this research.

References

Abraham-Shrauner, B., J. R. Asbridge, S. J. Bame, and W. C. Feldman, Proton-driven electromagnetic instabilities in high-speed solar wind streams, J. Geophys. Res., 84, 553, 1979.

Barnes, A., Hydromagnetic waves and turbulence in the solar wind, in Solar System Plasma Physics, Vol. 1, p. 249, C. F. Kennel, L. J. Lanzerotti, and E. N. Parker, editors, North-Holland, 1979.

Barnes, A., Theory of generation of bow-shock-associated waves in the upstream interplanetary medium, Cosmic Elec., 1, 90, 1970.

Batchelor, G. K., Theory of Homogeneous Turbulence, Cambridge Univ. Press, 1970.

Behannon, K. V., M. H. Acuna, L. F. Burlaga, R. P. Lepping, N. F. Ness, and F. M. Neubauer, Magnetic field experiment for Voyagers 1 and 2, Space Sci. Rev., 21, 235, 1977.

Bonifazi, C., and G. Moreno, Reflected and diffuse ions backstreaming from the earth's bow shock, 2, Origin, J. Geophys. Res., 86, 4405, 1981.

Boyd, T. J. M, and J. J. Sanderson, Plasma Dynamics, Barnes & Noble, Inc., New York, 1969.

Bridge, H. S., J. W. Belcher, R. J. Butler, A. J. Lazarus, A. M. Mauretic, J. D. Sullivan, G. L. Siscoe, and V. M. Vasyliunas, The plasma experiment on the 1977 Voyager mission, Space Sci. Rev., 21, 259, 1977.

Dawson, J., and I. B. Bernstein, Hydromanetic instabilities caused by runaway electrons, Controlled Thermonuclear Conference, Rep. AED-TID-7558, p. 360, Dep. of Commer., Washington, D. C., 1958.

Gary, S. P., The electromagnetic ion beam instability and energy loss of fast alpha particles, Nucl. Fusion, 18, 327, 1978.

Gary, S. P., J. T. Gosling, and D. W. Forslund, The electromagnetic ion beam instability upstream of the earth's bow shock, J. Geophys. Res., 86, 6691, 1981.

Hoppe, M. M., and C. T. Russell, Plasma rest frame frequencies and polarizations of the low-frequency upstream waves: ISEE 1 and 2 Observations, J. Geophys. Res., 88, 2021, 1983.

Hoppe, M. M., C. T. Russell, L. A. Frank, T. E. Eastman, and E. W. Greenstadt, Upstream hydromagnetic waves and their association with backstreaming ion populations: ISEE 1 and 2 observations, J. Geophys. Res., 86, 4471, 1981.

Kennel, C. F., and H. V. Wong, Resonant particle instabilities in a unifrom magnetic field, Plasma Phys., 1, 75, 1967.

Lee, M., Coupled hydromagnetic wave excitation and ion acceleration upstream of the earth's bow shock, J. Geophys. Res., 87, 5063, 1982.

Leroy, M. M., D. Winske, C. C. Goodrich, C. S. Wu, and K. Papadopoulos, The structure of perpendicular bow shocks, J. Geophys. Res., 87, 5081, 1982.

Matthaeus, W. H., and M. L. Goldstein, Measurement of the rugged invariants of magnetohydrodynamic turbulence in the solar wind, J. Geophys. Res., 87, 6011, 1982a.

Matthaeus, W. H., and M. L. Goldstein, Stationarity of magnetohydrodynamic fluctuations in the solar wind, J. Geophys. Res., 87, 10347, 1982b.

Moffatt, H. K., Magnetic Field Generation in Electrically Conducting Fluids, Cambirdge Univ. Press, 1978.

Montgomery, M. D., S. P. Gary, D. W. Forslund, and W. C. Feldman, Electromagnetic ion-beam instabilities in the solar wind, Phys. Rev. Lett., 35, 667, 1975.

Montgomery, M. D., S. P. Gary, W. C. Feldman, and D. W. Forslund, Electromagnetic instabilities driven by unequal proton beams in the solar wind, J.

Geophys. Res., 81, 2743, 1976.

Paschmann, G., N. Sckopke, I. Papamastorakis, J. R. Asbridge, S. J. Bame, and J. T. Gosling, Characteristics of reflected and diffuse ions upstream from the earth's bow shock, J. Geophys. Res., 86, 4355, 1981.

Paschmann, G., N. Sckopke, J. R. Asbridge, S. J. Bame, and J. T. Gosling, Energization of solar wind ions by relection from the earth's bow shock, J. Geophys. Res., 85, 4689, 1980.

Smith, C. W., M. L. Goldstein, and W. H. Mattheaus, Turbulence analysis of the Jovian upstream "wave" phenomenon, J. Geophys. Res., in press, 1983.

Smith, E. J., B. T. Tsurutani, D. L. Chenette, T. F. Conlon, and J. A. Simpson, Jovian electron bursts: Correlation with the interplanetary field direction and hydromagnetic waves, J. Geophys. Res., 81, 65, 1976.

Stix, T. H., The Theory of Plasma Waves, McGraw-Hill, New York, 1962.

Tademaru, E., Plasma instabilities of streaming cosmic rays, The Astrophys. J., 185, 959, 1969.

Tanaka, M., C. C. Goodrich, D. Winske, and K. Papadopoulos, A source of the backstreaming ion beams in the foreshock region, J. Geophys. Res., in press, 1983.

Table 1

Proton Density = 0.25/cm^3, Electron Temperature = 2 eV, Isothermal Approximation ($\gamma = 1$), $\langle B_o \rangle$(nT) = 0.33, C_s (cm/s) = 1.39×10^6, V_A (cm/s) = 1.44×10^6, V_{sw} (cm/s) = 4.19×10^7

n	Freq (mHz)	SW Freq (mHz)	θ (deg)	ϕ (deg)	V_{ph}(Fast) (km/s)	V_n/V_{sw}
1	1.52	6.32×10^{-2}	6.1	35.0	14.9	-2.8
1	1.71	6.97×10^{-2}	10.6	30.4	15.4	-2.8
1	1.89	7.71×10^{-2}	12.2	28.7	15.6	-2.5
1	2.08	8.51×10^{-2}	10.5	30.3	15.4	-2.2
1	2.27	9.33×10^{-2}	10.6	30.7	15.4	-2.0
1	2.46	0.10	10.8	30.3	15.4	-1.8
1	2.65	0.11	11.6	29.2	15.5	-1.7
1	2.84	0.11	16.7	24.4	16.1	-1.7
1	3.03	0.12	18.4	22.7	16.2	-1.6
1	3.22	0.13	17.5	23.5	16.1	-1.5
2	4.74	0.20	32.7	16.9	17.6	-2.5
2	4.92	0.21	35.8	12.2	17.8	-2.5
2	5.11	0.21	37.2	6.3	17.9	-2.6
2	5.30	0.22	37.4	5.9	17.9	-2.4
2	5.49	0.23	37.7	5.7	18.0	-2.4
2	5.68	0.24	39.1	5.3	18.1	-2.3
2	5.87	0.24	39.4	6.0	18.1	-2.3
2	6.06	0.25	39.8	5.5	18.1	-2.2
2	6.25	0.26	42.0	7.4	18.3	-2.2
2	6.44	0.27	42.2	7.8	18.3	-2.1
2	6.63	0.28	43.4	8.1	18.4	-2.1
2	6.82	0.29	41.4	4.9	18.2	-2.0
2	7.01	0.29	42.7	3.3	18.3	-2.0
2	7.20	0.30	39.4	2.0	18.1	-1.8
2	7.39	0.30	36.8	4.4	17.9	-1.7
2	7.58	0.31	36.8	7.9	17.9	-1.7
3	8.52	0.34	27.0	14.9	17.1	-2.0
3	8.71	0.35	30.3	10.6	17.4	-2.0
3	8.90	0.36	34.2	6.9	17.7	-2.1
3	9.09	0.37	36.9	3.9	17.9	-2.1
3	9.28	0.38	38.6	2.4	18.0	-2.1
3	9.47	0.39	37.5	3.6	17.9	-2.0
4	11.74	0.49	36.0	11.4	17.8	-2.1
4	11.93	0.50	36.3	12.0	17.8	-2.1
4	12.12	0.50	35.1	12.2	17.7	-2.0
4	12.31	0.51	35.5	11.6	17.8	-2.0
4	12.50	0.52	36.9	12.5	17.9	-2.0
4	12.69	0.53	34.7	12.7	17.7	-1.9
4	12.88	0.54	34.1	14.0	17.7	-1.9
4	13.07	0.55	29.8	19.3	17.3	-1.7

Table 2

Growth Rate calculations for the fast magnetosonic and Alfven modes

Electromagnetic ion beam instability

The computed growth rates have been maximized with respect to both $|\underline{k}|$ and propagation direction θ. Landau damping by thermal protons and electrons is included.

Proton Density = 0.25/cm³, Solar Wind Electron and Proton Temperatures = 2 eV, (used in Landau damping calculation), $\langle \underline{B}_o \rangle$(nT) = 0.33, V_A (cm/s) = 1.44×10^6, V_{sw} (cm/s) = 4.2×10^7

Fast Mode

n	$(\gamma/\Omega_p)_{max}$	SW Freq (mHz)	θ (deg)	V_{ph}/V_A	Deg.-Polarization
1*	0.428	1.96*	0	20.2	1.0
2	0.473	0.24	31	1.0	0.18
3	0.148	0.38	35	1.0	0.23
4	0.060	0.50	34	1.0	0.30

* Calculated by solving simultaneously for the real and imaginary parts of the frequency [cf. Lee, 1982]. The large value of the plasma frame frequency suggests that the ratio n_b/n_o should be chosen to be less than 0.01.

Alfven Mode

n	$(\gamma/\Omega_p)_{max}$	SW Freq (mHz)	θ (deg)	V_{ph}/V_A	Deg.-Polarization
1**					
2	0.82	0.20	48	0.67	-0.035
3	0.38	0.30	48	0.67	-0.052
4	0.22	0.40	48	0.66	-0.069

** For the Alfven mode, $(\gamma/\Omega_p)_{max} = 0$ at $\theta = 0$, but reaches a maximum value greater than 1 (but still less than the off-angle maximum for the fast mode) at 32°.

Appendix A

In the limit $\gamma \ll \Omega_p$, the growth rate of low frequency MHD waves as computed from the linearized Vlasov-Maxwell equations is given by [Stix, 1962; Kennel and Wong, 1967; Tademaru, 1969]

$$\gamma = -R^i/(\partial R^r/\partial\omega) \tag{A1}$$

where R^r is the real part of the determinant of the dispersion tensor, in this case computed in the cold plasma approximation [cf. Stix, 1962], and R^i is the imaginary part of the determinant of the dispersion tensor, which includes the suprathermal streaming proton component. The components comprising R^i can be found in, for example, Stix [1962]. When substituted into (A1) the result is [Kennel and Wong, 1967; Tademaru, 1969]

$$\gamma = -2\pi^2[(R^r_{11}R^r_{33}-(R^r_{13})^2)(\partial R^r/\partial\omega)^{-1}\frac{\omega}{k_\parallel}\,\mathrm{sgn}(k_\parallel)$$

$$\times \sum_\alpha \omega_\alpha^2 \int_0^\infty dv_\perp\, v_\perp^2\,[\frac{\partial f_\alpha}{\partial v_\perp} + \frac{k_\parallel}{\omega}(v_\perp\frac{\partial f_\alpha}{\partial v_\parallel} - v_\parallel\frac{\partial f_\alpha}{\partial v_\perp})]$$

$$\times \sum_n [R^r_{33}R^r_{12}(n/\lambda)J_n(\lambda) - R^r_{12}R^r_{13}(v_\parallel/v_\perp)J_n(\lambda) -$$

$$(R^r_{11}R^r_{33} - (R^r_{13})^2)J_n'(\lambda)]^2 \Big|_{v_\parallel=(\omega-n\Omega_\alpha)/k_\parallel}$$

(A2)

where $\omega_\alpha^2 = 4\pi ne^2/m_\alpha$ is the square of the plasma frequency of species α, $\lambda = v_\perp k_\perp/\Omega_\alpha$, is the argument of the Bessel functions J_n (' denotes differentiation

with respect to λ), $\Omega_\alpha = \zeta eB/m_\alpha c$ is the Larmor frequency of species α ($\zeta = +1$ for ions and -1 for electrons), the sum over n ranges from $-\infty$ to $+\infty$ and the sum over α includes both protons and electrons. R is the determinant of R^r_{ij}. The components of R^r_{ij} used in (A2) are

$$R^r_{11} = k_\parallel{}^2c^2 - \omega^2 + \Sigma \frac{\omega_\alpha{}^2\omega^2}{\omega^2 - \Omega_\alpha{}^2}$$

$$R^r_{12} = \omega \Sigma \frac{\omega_\alpha{}^2\omega^2}{\omega^2 - \Omega_\alpha{}^2}$$

$$R^r_{22} = k^2c^2 - \omega^2 + \Sigma \frac{\omega_\alpha{}^2\omega^2}{\omega^2 - \Omega_\alpha{}^2}$$

$$R^r_{13} = -k_\perp k_\parallel c^2$$

$$R^r_{33} = k_\perp{}^2c^2 - \omega^2 + \Sigma\omega_\alpha{}^2 \qquad \text{(A3)}$$

where the summation is over the cold plasma population (protons and electrons).

Appendix B

When a conical distribution of wave numbers is integrated to form the reduced spectrum, the magnitude of the spread in the spectral peaks can be estimated in a fairly straightforward way. We have considered a model wave spectrum of the form

$$E(\underline{\kappa}) = (E_o/2\pi\kappa_\perp)\ \delta(\underline{k}_\perp-\underline{\kappa}_\perp)\ \delta(k_\parallel-\kappa_\parallel) \tag{B1}$$

where the resonant wavevectors are the set $\underline{k} = (\underline{k}_\perp, k_\parallel)$. The reduced spectrum $E_r(k_R)$ is obtained by integrating the spectrum over all wavevectors with a fixed radial projection k_R, that is,

$$E_r(k_R) = \int E(\underline{\kappa})\ \delta(\underline{\kappa}\cdot\underline{R} - k_R)\ d^3\kappa. \tag{B2}$$

The integral can be easily performed by changing variables. After a little algebra we find

$$E_r(k_R) = (E_o/\pi)\ 1/\sqrt{[k_\perp^2\sin^2\theta - (k_R - k_\parallel\cos\theta)^2]} \tag{B3a}$$

for $|k_R-k_\parallel\cos\theta| \leq k_\perp\sin\theta$, and

$$E_r(k_R) = 0 \tag{B3b}$$

otherwise. In (B3), θ is the angle between the axis of the cone and the magnetic field.

The reduced spectrum consists of two peaks, symmetrically spaced about k_R

$= k_{\parallel}\cos\theta$. The upper peak occurs at $k_R = k_{\parallel}\cos\theta + k_{\perp}\sin\theta$ and the lower at $k_R = k_{\parallel}\cos\theta - k_{\perp}\sin\theta$. In the special case of $k_{\perp} = k_{\parallel}$ and $\theta = 45^{\circ}$, the lower peak is at zero wavenumber and does not contribute to the fluctuation spectrum while the upper peak is at $k_R = k = \sqrt{(k_{\perp}^2 + k_{\parallel}^2)}$ which is the exact resonant wavenumber. It appears that the spectral smoothing obtained from a reduced spectrum still retains, at the approximate resonant wavenumbers, the spectral peaks of the three dimensional spectrum.

Figure Captions

Figure 1. Magnetometer data from the GSFC experiment on Voyager 2. The time span shown is from about 9:00 - 10:30 UT on day 184 of 1979. The data are 9.6 sec averages and have been rotated into a field aligned coordinate system in which z is in the direction of the mean field and x is in the original R-T plane. The y-component then completes the right-handed coordinate system.

Figure 2. a. The trace of the magnetic power spectral matrix for this interval. The power is in $(nT)^2$. The spectrum was obtained using the fast Fourier transform technique with 14 degrees of freedom. The data consisted of 1.92 sec averages of the field. It was digitally filtered using a low-pass filter which removed aliasing at the highest frequencies.

b. The power in the magnitude of the magnetic field. This spectrum was obtained as described for Fig. 2a.

Figure 3. The normalized magnetic helicity spectrum, $\sigma_m(f)$ after Matthaeus and Goldstein [1982a].

Figure 4. The results of an eigenvalue analysis of this interval. Plotted in panels a through c are the degree of polarization D, the ellipticity ϵ, and the angle θ between B_o and $\underline{k}$, respectively.

Figure 5. a. The correlation between $|B(f)|$ and $\rho(f)$ [see Smith et al., 1983].

b. The normalized cross helicity spectrum, $\sigma_c(f)$ after Matthaeus and Goldstein [1982a].

c. The Alfven ratio $r_A = E_V(f)/E_B(f)$ where $E_V(f)$ and $E_B(f)$ are the spectra of kinetic and magnetic energy, respectively.

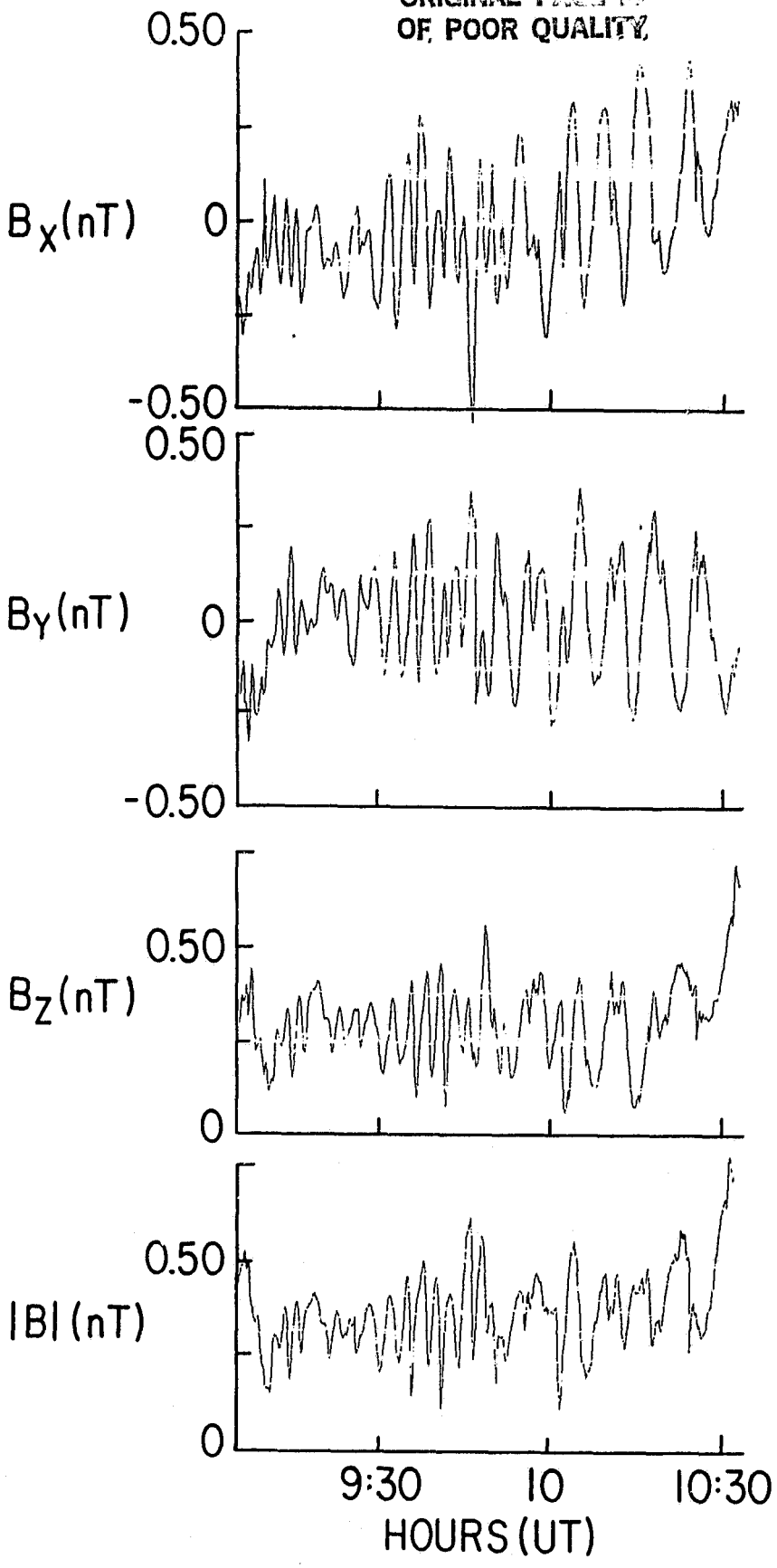

Figure 1

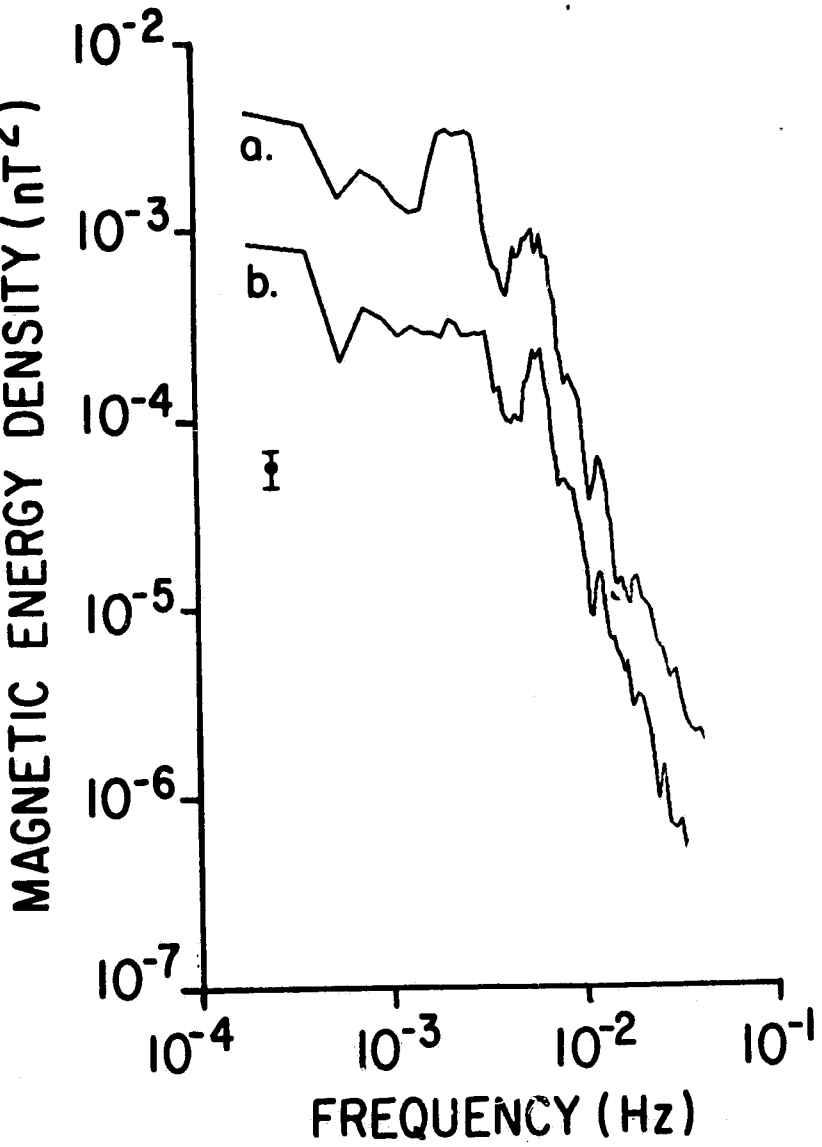

Figure 2

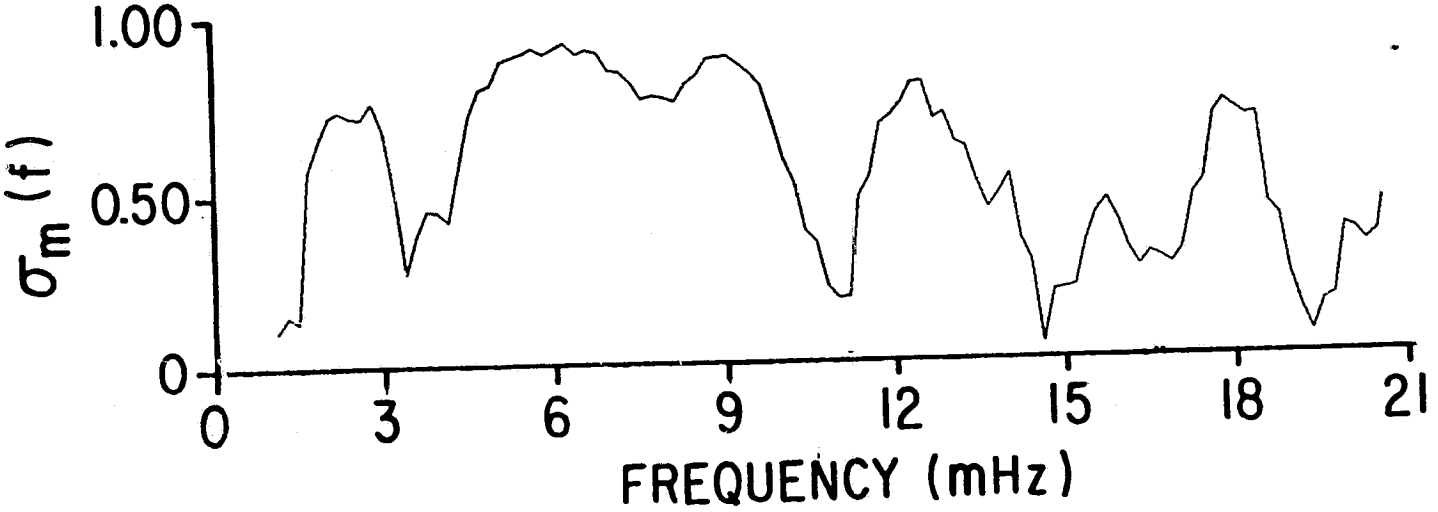

Figure 3

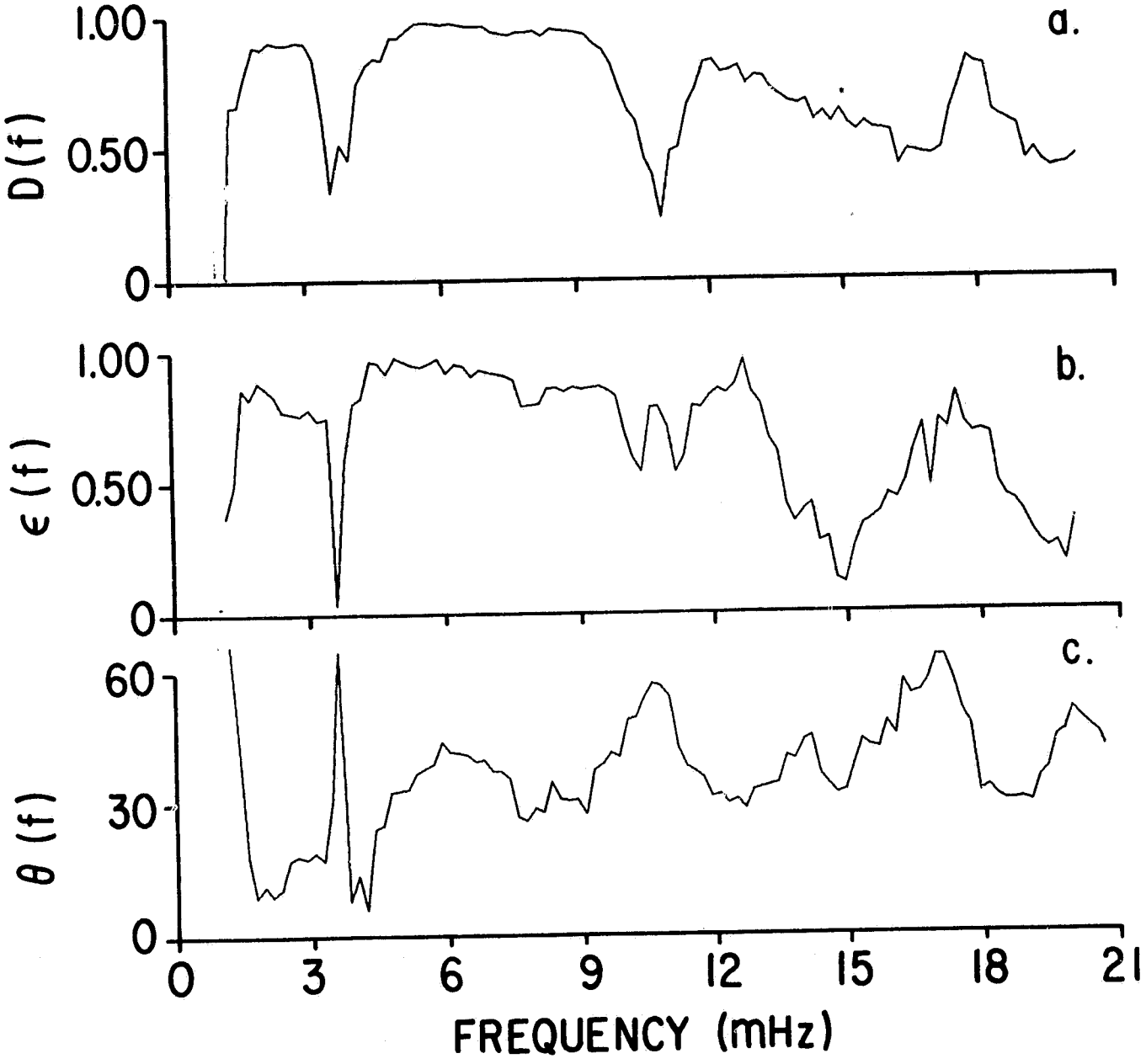

Figure 4

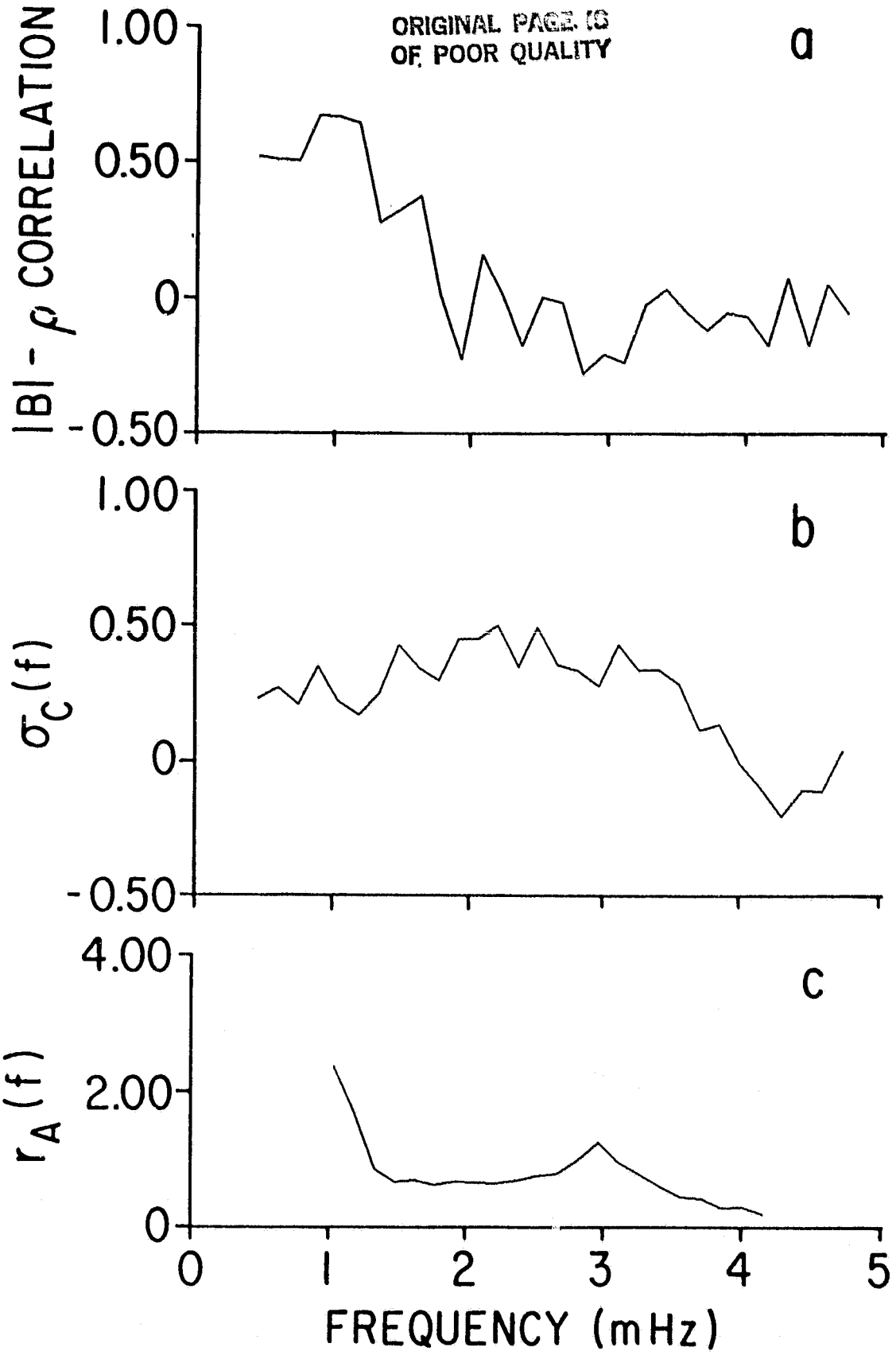

Figure 5